The usefulness of image-enhanced endoscopy to distinguish gastric carcinoma in tumors initially diagnosed as adenomas by endoscopic biopsy
A retrospective study

Yuhei Umeda, MD[a,b,c], Kyosuke Tanaka, MD, PhD[a,b,*] (iD), Yohei Ikenoyama, MD, PhD[a,b],
Yasuhiko Hamada, MD, PhD[b], Hiroki Yukimoto, MD, PhD[b], Reiko Yamada, MD, PhD[b],
Junya Tsuboi, MD[a,b], Misaki Nakamura, MD, PhD[a], Masaki Katsurahara, MD, PhD[a], Noriyuki Horiki, MD, PhD[b],
Toru Ogura, PhD[d], Satoshi Tamaru, MD, PhD[d], Hayato Nakagawa, MD, PhD[a,b], Isao Tawara, MD, PhD[c]

Abstract

Superficial epithelial gastric neoplasms can be divided into adenomas and early carcinomas. Histological diagnosis by endoscopic forceps biopsy is crucial for the diagnosis and management of gastric neoplasms. It is difficult to distinguish features of gastric neoplasms in small biopsy specimens; hence, gastric carcinomas can be underdiagnosed as adenomas. Recent developments in image-enhanced endoscopy have improved the ability to differentiate between carcinomatous and non-carcinomatous lesions. To investigate the prevalence of gastric carcinoma in lesions initially diagnosed as adenomas by forceps biopsy and assess the usefulness of image-enhanced endoscopy in distinguishing carcinomas. A total of 142 lesions of gastric adenomas, diagnosed by biopsy and resected endoscopically between January 2010 and May 2020, were retrospectively evaluated. Images were captured by white-light endoscopy (WLE), magnifying endoscopy with narrow-band imaging (M-NBI), and magnifying endoscopy with acetic acid and narrow-band imaging (M-AANBI); they were analyzed and compared with histopathological results. The diagnostic performance of M-AANBI was compared with that of M-NBI. Of the 142 lesions, 58 (40.8%) were pathologically diagnosed as adenocarcinomas. On WLE images, a depressed macroscopic type and size ≥20 mm were significant predictors of carcinoma ($P < .001$); however, they displayed low sensitivities (32.8% and 41.4%, respectively). M-AANBI displayed significantly higher sensitivity, specificity, and accuracy for distinguishing carcinomas than M-NBI (94.8% vs 74.1%, 81.0% vs 72.6%, and 86.6% vs 73.2%, $P < .05$). In conclusion, carcinoma was prevalent in 40.8% of gastric lesions initially diagnosed as adenomas by forceps biopsy. M-AANBI may be more useful than M-NBI and WLE in distinguishing gastric carcinomas from adenomas.

Abbreviations: CI = confidence interval, ESD = endoscopic submucosal dissection, M-AA = magnifying endoscopy with acetic acid, M-AANBI = magnifying endoscopy with acetic acid and narrow-band imaging, M-NBI = magnifying endoscopy combined with narrow-band imaging, OR = odds ratio, WLE = white-light endoscopy.

Keywords: acetic acid, endoscopy, narrow band imaging, stomach neoplasms

1. Introduction

Superficial epithelial gastric neoplasms can be divided into adenomas and early carcinomas. Adenomas have a lower risk of progression than early carcinomas.[1] Therefore, an accurate diagnosis of a lesion is important for appropriate management.

Histological diagnosis by endoscopic forceps biopsy is crucial for the diagnosis and management of gastric neoplasms.

However, it is occasionally difficult to identify the features of entire gastric neoplasms based on small biopsy specimens.[2,3] Thus, gastric carcinomas are often underdiagnosed. The prevalence of carcinoma after the resection of adenomas ranges between 16.1% and 55.3%.[4–8] The difference in pathological diagnosis before and after endoscopic resection of gastric lesions diagnosed as adenomas by forceps biopsy is of particular concern. An improper follow-up strategy for gastric adenomas

may result in a missed opportunity for endoscopic treatment. This necessitates an accurate preoperative diagnosis to select an appropriate management strategy. In white-light endoscopy (WLE), certain characteristics of gastric adenomas, like large size, red color, and depressed type, are recognized as significant predictive factors of malignancy.[4–8] However, WLE findings have low accuracy, thus warranting a more accurate diagnostic method.

Recent developments in image-enhanced endoscopic techniques have improved the ability to differentiate between carcinomatous and non-carcinomatous lesions. Magnifying endoscopy combined with narrow-band imaging (M-NBI) enables the visualization of microvascular and microsurface patterns on the gastric mucosa.[9–11] Previously, magnifying endoscopy with acetic acid (M-AA) enabled clear visualization of the mucosal microsurface patterns in gastric neoplasms.[12,13] Further, M-AA and NBI (M-AANBI) have been reported as practical diagnostic procedures for gastric neoplasms.[14]

In this study, we aimed to investigate the prevalence of gastric carcinoma in lesions initially diagnosed as adenomas by forceps biopsy and to evaluate the usefulness of M-NBI and M-AANBI to differentiate between gastric carcinoma and adenomas.

2. Methods

2.1. Patients

This retrospective study was conducted at a single endoscopy unit at Mie University Hospital in Japan. We enrolled 134 consecutive patients with 158 gastric adenomas diagnosed by forceps biopsy and resected endoscopically between January 2010 and May 2020. Furthermore, all lesions were treated by endoscopic submucosal dissection (ESD) following preoperative M-NBI/M-AANBI. Almost all gastric lesions were always resected by ESD at our hospital because of its high complete resection rate. Of these, 16 lesions were excluded because 15 did not undergo M-AANBI procedures, and one generated only low-quality images. Hence, we analyzed 125 patients with 142 lesions (Fig. 1). This study conformed to the tenets of the Declaration of Helsinki as reflected by the approval of the medical ethics committee of Mie University Hospital (H2020-204). Informed consent was obtained from all patients in an opt-out form on the website.

2.2. Endoscopic procedure

After being initially diagnosed with gastric adenoma by biopsy, all patients underwent detailed endoscopy before endoscopic resection. All endoscopic procedures were performed using a magnifying endoscope (GIF-Q240Z, GIF-H260Z, or GIF-H290Z, Olympus Co., Tokyo, Japan) and an endoscopic system with NBI (EVIS LUCERA ELITE or EVIS LUCERA SPECTRUM, Olympus Co.). A distal attachment (MAJ-1989 or MAJ-1990, Olympus Co.) was fitted on the tip of the endoscope to stabilize it and maintain a suitable focusing distance during all magnified observations.

All endoscopic procedures were performed at the Mie University Hospital, and all endoscopic images were obtained using the following steps: the gastric lesion was detected by WLE at the beginning of a procedure, and representative WLE images were obtained for evaluating macroscopic characteristics, such as the macroscopic type, tumor size, and surface color. Subsequently, WLE was switched to NBI, and M-NBI images were obtained to evaluate a lesion demarcation line as well as microvascular and microsurface patterns. At low pressure, 1.5% acetic acid was added to the lesion with a 20 mL syringe through the accessory channel of the endoscope, and M-AANBI images were obtained to evaluate the microsurface patterns (See Video S1, Supplemental Digital Content, http://links.lww.com/MD/I439, which demonstrates the M-AANBI procedure). All lesions were eventually resected en bloc by ESD without any complications.

2.3. Endoscopic imaging evaluation

The images obtained by WLE, M-NBI, and M-AANBI were evaluated by 2 endoscopists (YU and KT) for tumor location, macroscopic type (elevated or depressed), tumor size (<20 mm or ≥20 mm), color (whitish or reddish), and M-NBI/M-AANBI findings (Fig. 2). Any disagreement was resolved by discussion. The precise tumor size was measured using the resected specimen, and its mean value was derived. On WLE images, a depressed macroscopic type, large size (≥20 mm), and reddish color within lesions were separately defined as predictive factors of carcinoma. We evaluated M-NBI images using the algorithm for early gastric carcinoma diagnosis by magnifying endoscopy.[15] Lesions with irregular microvascular or microsurface patterns were predicted to be carcinomatous. Other lesions were diagnosed as non-carcinomatous adenomas. A distinct demarcation line between the lesion and adjacent mucosa was essential
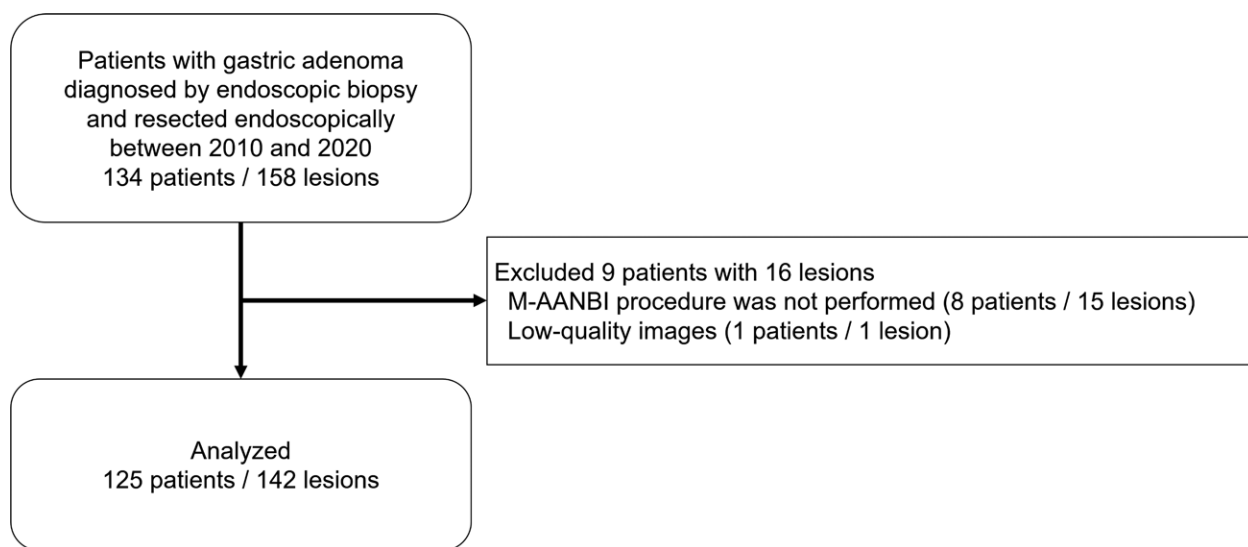

Figure 1. Flowchart depicting the enrollment of patients with lesions.

for carcinoma diagnosis based on this algorithm. Despite being moderately unclear compared to that in definite carcinoma, a demarcation line was also necessary for adenoma diagnosis.

The findings from M-AANBI were also evaluated using a microsurface pattern classification based on previous reports.[12,13] Gastric mucosal microsurface patterns by M-AA and M-AANBI are almost identical and are classified into 5 types as follows: small round pits, slit, gyrus/villous, irregular, and destructive. The slit and gyrus/villous patterns are common in gastric adenoma and the irregular pattern in differentiated adenocarcinoma (Fig. 3). Based on this classification, an irregular pattern was considered predictive of carcinoma even if it involved a small area. Thus, lesions with irregular and slit patterns or gyrus/villous patterns were diagnosed as carcinomatous. Contrarily, they were predicted to be adenomas upon observing slit and gyrus/villous patterns without irregular patterns. In cases of mixed patterns with slit and gyrus/villous patterns, we considered the dominant pattern.
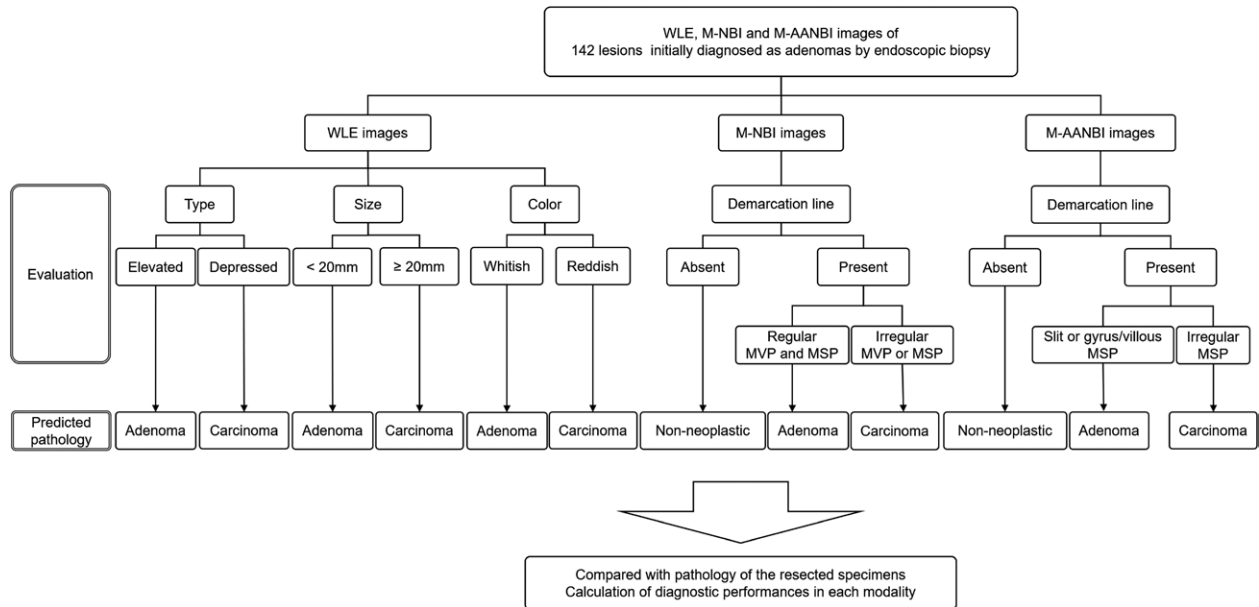
Figure 2. A diagnostic algorithm for each endoscopic modality. M-AANBI = magnifying endoscopy with acetic acid and narrow-band imaging, M-NBI = magnifying endoscopy with narrow-band imaging, MSP = microsurface pattern, MVP = microvascular pattern, WLE = white-light endoscopy.
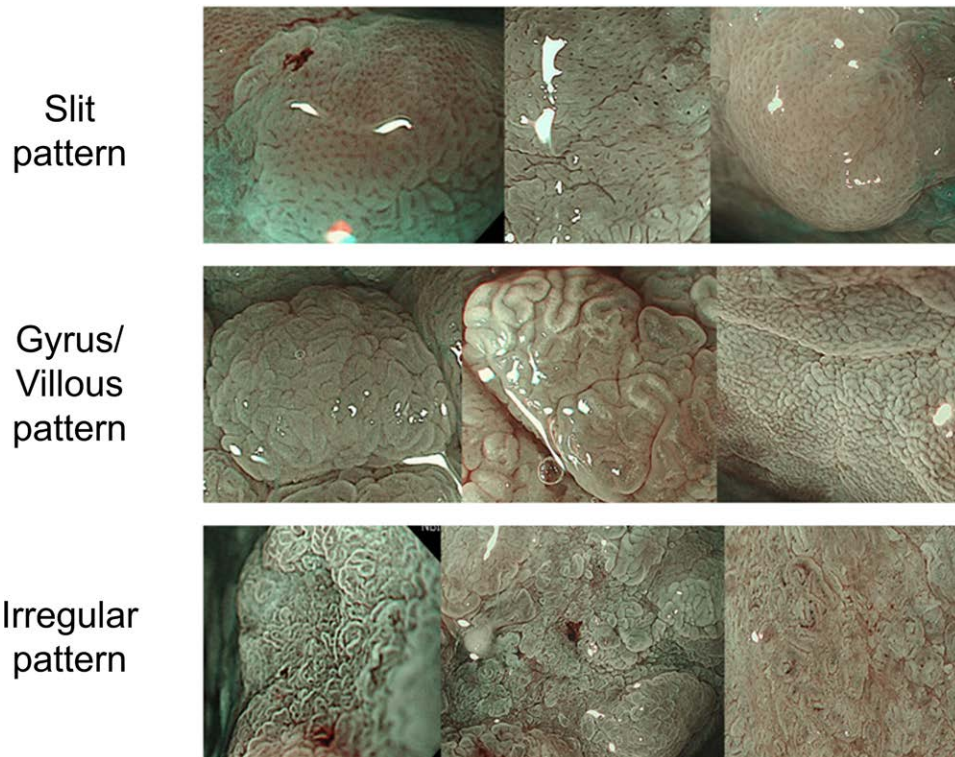
Figure 3. Surface patterns of neoplastic lesions (adenomas or carcinomas) using magnifying endoscopy with acetic acid and narrow-band imaging are classified into 3 types, namely, slit, gyrus/villous, and irregular. Slit and gyrus/villous patterns indicate adenoma. Irregular patterns indicate carcinoma.

2.4. Histopathological evaluation

Each resected specimen was cut into 2 mm slices after fixation in formalin, and the histological type, size, tumor depth, and lymphovascular invasion were evaluated. A pathological diagnosis (adenoma or carcinoma) based on hematoxylin-eosin staining was made by 2 expert pathologists blinded to the endoscopic findings. The depth of tumor invasion was recorded using its T category. T1a and T1b were defined as tumors confined to the mucosa or submucosa, respectively.[16] T1b was further divided into T1b1 and T1b2 for tumors that displayed marginal submucosal invasion confined within 0.5 mm from the muscularis mucosae and submucosal invasion ≥0.5 mm, respectively.

2.5. Statistical analyses

Continuous variables are summarized as mean ± standard deviation, whereas categorical variables are summarized as frequencies and percentages. We assessed the clinical and endoscopic characteristics, including sex, age, macroscopic type, lesion location, maximal diameter, color, invasion depth, and M-NBI and M-AANBI findings. The localized site was classified as upper, middle, or lower, according to the lines connecting the trisected points on the lesser and greater curvatures and based on the Japanese classification of gastric carcinoma.[16] Student t test was performed to analyze differences in the continuous variables, such as age and size. Fisher exact test was conducted for all categorical variables. We determined a 95% confidence interval (CI) for comparing the sensitivity, specificity, and accuracy of WLE, M-NBI, and M-AANBI using McNemar test. Univariate and multivariable logistic regression analyses were used to determine the significant factors contributing to the diagnosis of gastric carcinoma. Variables showing a significant association in the univariate analysis were included in the multivariate logistic regression analysis. Statistical significance was set at $P < .05$.

The kappa value (κ value) was calculated to assess image evaluation using M-AANBI. Agreement between the observers was quantified using Cohen kappa coefficients. Of the 142 consecutive lesions, 142 images were obtained using M-AANBI and used for the agreement test. Two experts for M-AANBI (YH and MK) and 2 non-experts (YI and MN) evaluated the microsurface patterns (slit, gyrus/villous, irregular) and their diagnoses (adenoma vs carcinoma) for each image after attending a lecture on M-AANBI. We defined experts as those who had performed more than 100 M-AANBI procedures for gastric neoplasms. The strength of each agreement was graded by the κ value (slight: 0.01–0.2, fair: 0.21–0.4, moderate: 0.41–0.6, substantial: 0.61–0.8, and almost perfect: 0.81–1.0).

Statistical analysis was performed using IBM SPSS Statistics version 25 (IBM Corp., Chicago, IL) and EZR version 1.51 (Saitama Medical Center, Jichi Medical University, Japan).[17]

3. Results

3.1. Clinical characteristics

A total of 125 patients with 142 lesions were included in this study; Table 1 summarizes their clinical characteristics. The patients were predominantly men (93 men and 32 women), and the mean age was 71.6 ± 9.25 years (range: 41–89). Regarding *Helicobacter pylori* (Hp) infection status, 54 and 88 lesions were observed in patients with a positive Hp infection and Hp eradication history, respectively. All patients had a history of Hp infection. Eleven, 50, and 81 lesions were located in the upper third, middle third, and lower third sections of the stomach, respectively. The majority of lesions (81.0%, n = 115) were elevated macroscopic type, and 27 (19.0%) were depressed. The mean tumor size was 16.0 ± 9.68 mm (range: 2–48). Fifty-one lesions (35.9%) were whitish, and the remaining 91 (64.1%) were reddish. All lesions were resected en bloc using ESD. More than half of the lesions (59.2%, n = 84)

were histopathologically diagnosed as adenomas, and the remaining (40.8%, n = 58) were well-differentiated adenocarcinomas. Among the diagnosed carcinomas, the depth of invasion of lesions showed 55 for T1a, 1 for T1b1, and 2 for T1b2.

3.2. WLE evaluation and histopathological characteristics

Table 1 summarizes the associations between macroscopic WLE findings and histopathological characteristics. Table 2 summarizes the diagnostic performance of each predictive factor for carcinoma. The frequency of depressed macroscopic lesions was significantly higher in carcinomas than in adenomas (32.8% vs 9.5%, $P < .001$). The diagnostic performance of the depressed macroscopic type for gastric carcinoma was as follows: sensitivity, 32.8% (95% CI: 21.0%–46.3%); specificity, 90.5% (95% CI: 82.1%–95.8%); and accuracy, 66.9% (58.5%–74.6%). Carcinomas were significantly larger than adenomas ($P < .001$). Moreover, the frequency of lesions ≥ 20 mm in size was significantly higher among carcinomas than among adenomas (41.4% vs 15.5%, $P < .001$). The diagnostic performance of tumor size (≥20 mm) for gastric carcinoma was as follows: sensitivity, 41.4% (95% CI: 28.6%–55.1%); specificity, 84.5% (95% CI: 75.0%–91.5%); and accuracy, 66.9% (95% CI: 58.5%–74.6%). Pathological results between whitish and reddish lesions indicated borderline statistical significance, although the frequency of the former was higher in carcinomas compared to adenomas (74.1% vs 57.1%, $P = .0501$). The diagnostic performance of reddish color for gastric carcinoma was as follows: sensitivity, 74.1% (95% CI: 61.0%–84.7%); specificity, 42.9% (95% CI: 32.1%–54.1%); and accuracy, 55.6% (95% CI: 47.1%–64.0%). Table 2 summarizes the diagnostic performances of any combinations of WLE findings. All diagnostic performances of WLE, especially accuracies, were insufficient compared to those of M-NBI and M-AANBI.

3.3. M-NBI evaluation and histopathological characteristics

Table 1 summarizes the associations between M-NBI findings and histopathological characteristics. All lesions displayed observable demarcation lines. A total of 66 lesions had irregular microvascular and/or microsurface patterns. Of these, 43 lesions were identified as carcinomas in the final histopathological results. Thus, the frequency of irregular microvascular/microsurface patterns was significantly higher in carcinomas than in adenomas (74.1% vs 27.4%, $P < .001$). According to the M-NBI diagnosis, its diagnostic sensitivity, specificity, and accuracy for distinguishing carcinomas from adenomas were 74.1% (95% CI: 61.0%–84.7%), 72.6% (95% CI: 61.8%–81.8%), and 73.2% (95% CI: 65.2%–80.3%), respectively (Table 2).

3.4. M-AANBI evaluation and histopathological characteristics

Table 1 depicts the associations between M-AANBI findings and histopathological characteristics. All lesions displayed demarcation lines. A mixed pattern with irregular and regular patterns (slit or gyrus/villous) was observed in 18 lesions (histopathologically, 3 adenomas and 15 adenocarcinomas) that were evaluated to have irregular patterns and endoscopically diagnosed as carcinomas. The frequency of the slit pattern was significantly higher in adenomas than in carcinomas (47.6% vs 0.0%, $P < .001$), similar to the frequency of the gyrus/villous pattern (33.3% vs 5.2%, $P < .001$). In comparison, the frequency of irregular patterns was significantly higher in carcinomas than in adenomas (94.8% vs 19.1%, $P < .001$). Both slit and gyrus/villous patterns were significant predictive factors for adenomas, similar to the irregular pattern for carcinomas. All lesions with slit patterns were histologically diagnosed as adenomas. For M-AANBI diagnosis, its diagnostic sensitivity,

Table 1

Clinicopathological characteristics of endoscopic findings.

| | Total | Pathology of the resected specimens | | P value |
		Adenoma	Carcinoma	
Patients	125	71	54	–
Sex (male/female)	93/32	48/23	45/9	.062
Age (mean ± SD)	71.6 ± 9.25	72.9 ± 8.39	70.4 ± 10.2	.099
Number of lesions (%)	142	84 (59.2)	58 (40.8)	–
Helicobacter pylori				.488
Positive, n (%)	54 (38)	34 (40.5)	20 (34.5)	
Eradicated, n (%)	88 (62)	50 (59.5)	38 (65.5)	
WLE: location				.002
Upper, n (%)	11 (7.8)	4 (4.8)	7 (12.0)	
Middle, n (%)	50 (35.2)	39 (46.4)	11 (19.0)	
Lower, n (%)	81 (57.0)	41 (48.8)	40 (69.0)	
WLE: macroscopic type				<.001
Elevated, n (%)	115 (81.0)	76 (90.5)	39 (67.2)	
Depressed, n (%)	27 (19.0)	8 (9.5)	19 (32.8)	
WLE: size (mean ± SD)	16.0 ± 9.68	12.9 ± 6.93	20.4 ± 11.4	<.001
<20 mm, n (%)	105 (73.9)	71 (84.5)	34 (58.6)	
≥20 mm, n (%)	37 (26.1)	13 (15.5)	24 (41.4)	
WLE: color				.0501
Whitish, n (%)	51 (35.9)	36 (42.9)	15 (25.9)	
Reddish, n (%)	91 (64.1)	48 (57.1)	43 (74.1)	
M-NBI				
Irregular MV pattern, n (%)	60 (42.3)	23 (27.4)	37 (63.8)	<.001
Irregular MS pattern, n (%)	55 (38.7)	18 (21.4)	37 (63.8)	<.001
Irregular MV and/or irregular MS pattern, n (%)	66 (46.5)	23 (27.4)	43 (74.1)	<.001
M-AANBI				
Slit pattern, n (%)	40 (28.2)	40 (47.6)	0 (0.0)	<.001
Gyrus/villous pattern, n (%)	31 (21.8)	28 (33.3)	3 (5.2)	<.001
Irregular pattern, n (%)	71 (50.0)	16 (19.1)	55 (94.8)	<.001
Depth of invasion				
T1a, n (%)	–	–	55 (94.9)	
T1b1, n (%)	–	–	1 (1.7)	
T1b2, n (%)	–	–	2 (3.4)	

– = not applicable, M-AANBI = magnifying endoscopy with acetic acid and narrow-band imaging, M-NBI = magnifying endoscopy with narrow-band imaging, MS = microsurface, MV = microvascular, SD = standard deviation, T1a = tumor confined to the mucosa, T1b1 = submucosal invasion < 0.5 mm, T1b2 = submucosal invasion ≥ 0.5 mm, WLE = white light endoscopy.

Table 2

Diagnostic performances of the predictive factors for gastric carcinoma on endoscopy.

Endoscopic findings	Sensitivity (95% CI)	Specificity (95% CI)	Accuracy (95% CI)
WLE: depressed macroscopic type	32.8% (21.0–46.3%)	90.5% (82.1–95.8%)	66.9% (58.5–74.6%)
WLE: size ≥ 20 mm	41.4% (28.6–55.1%)	84.5% (75.0–91.5%)	66.9% (58.5–74.6%)
WLE: reddish color	74.1% (61.0–84.7%)	42.9% (32.1–54.1%)	55.6% (47.1–64.0%)
WLE combinations of above findings			
One or more findings	87.9% (76.7–95.0%)	39.3% (28.8–50.5%)	59.2% (50.6–67.3%)
Depressed or size ≥ 20 mm	63.8% (50.1–76.0%)	75.0% (64.4–83.8%)	70.4% (62.2–77.8%)
Depressed or reddish	74.1% (61.0–84.7%)	41.7% (31.0–52.9%)	54.9% (46.4–63.3%)
Size ≥ 20 mm or reddish	87.9% (76.7–95.0%)	40.5% (29.9–51.7%)	59.9% (51.3–68.0%)
Two or more findings	50.0% (36.6–63.4%)	78.6% (68.3–86.8%)	66.9% (58.5–74.6%)
Depressed and size ≥ 20 mm	10.3% (3.90–21.2%)	100% (93.6–100%)	63.4% (54.9–71.3%)
Depressed and reddish	32.8% (21.0–46.3%)	91.7% (83.6–96.6%)	67.6% (59.2–75.2%)
Size ≥ 20 mm and reddish	27.6% (16.7–40.9%)	86.9% (77.8–93.3%)	62.7% (54.2–70.6%)
Three findings	10.3% (3.90–21.2%)	100% (93.6–100%)	63.4% (54.9–71.3%)
M-NBI	74.1% (61.0–84.7%)	72.6% (61.8–81.8%)	73.2% (65.2–80.3%)
M-AANBI	94.8%* (85.6–98.9%)	81.0%* (70.9–88.7%)	86.6%* (77.9–91.7%)

CI = confidence interval, M-AANBI = magnifying endoscopy with acetic acid and narrow-band imaging, M-NBI = magnifying endoscopy with narrow-band imaging, WLE = white light endoscopy.

* $P < .05$, McNemar test, vers M-NBI.

specificity, and accuracy for distinguishing carcinomas from adenomas were 94.8% (95% CI: 85.6%–98.9%), 81.0% (95% CI: 70.9%–88.7%), and 86.6% (95% CI: 79.9%–91.7%), respectively (Table 2). And Those of M-AANBI were significantly higher than those of M-NBI ($P < .05$).

In the univariate analysis, a depressed macroscopic type (odds ratio [OR] = 4.57, 95% CI: 1.73–13.2, $P < .001$), size ≥ 20 mm (OR = 3.82, 95% CI: 1.64–9.25, $P < .001$), and carcinomatous findings on either M-NBI or M-AANBI (OR = 47.0, 95% CI: 13.3–257, $P < .001$) were significantly associated with a carcinoma diagnosis (Table 3). No significant association was observed between the reddish color on WLE images and carcinoma diagnosis (OR = 2.14, 95% CI: 0.98–4.82, $P = .0501$).

Table 3

Univariate and multivariate analyses of predictive factors for gastric carcinoma.

Parameters	Univariate	Multivariate
Subgroups	OR (95% CI)	OR (95% CI)
Macroscopic type		
Depressed	4.57 (1.73–13.2)**	1.93 (0.59–6.34)
Elevated	1.0	1.0
Size		
≥20 mm	3.82 (1.64–9.25)**	3.63 (1.22–10.8)*
<20 mm	1.0	1.0
Color		
Reddish	2.14 (0.98–4.82)	1.37 (0.47–3.95)
Whitish	1.0	1.0
M-NBI/M-AANBI findings		
Carcinoma	47.0 (13.3–257)**	39.3 (10.7–145)**
Adenoma	1.0	1.0

CI = confidence interval, M-AANBI = magnifying endoscopy with acetic acid and narrow-band imaging, M-NBI = magnifying endoscopy with narrow-band imaging, OR = odds ratio.

* $P < .05$.

** $P < .01$.

In the multivariate analysis, size ≥ 20 mm (OR = 3.63, 95% CI: 1.22–10.8, $P = .020$) and carcinomatous findings on either M-NBI or M-AANBI (OR = 39.3, 95% CI: 10.7–145, $P < .001$) were significant factors associated with the diagnosis of carcinoma (Table 3).

The κ values were calculated for an inter-observer agreement on the microsurface patterns of M-AANBI and the diagnosis by 2 experts and 2 non-experts. Inter-observer agreements between the experts (YH and MK) were 0.67 and 0.72, respectively, and between the non-experts (YI and MN) were 0.69 and 0.76, respectively. This finding implied a substantial level of agreement.

3.5. The comparison of diagnostic values between M-NBI and M-AANBI

Fig. 4 depicts the comparison of diagnostic values between M-NBI and M-AANBI. Upon using M-NBI, 23 lesions were overdiagnosed and 15 were underdiagnosed. Upon using M-AANBI, 16 lesions were overdiagnosed and 3 were underdiagnosed. Nineteen lesions (7 adenomas and 12 carcinomas) misdiagnosed by M-NBI were correctly diagnosed by M-AANBI. The lesions diagnosed accurately by M-NBI were not misdiagnosed by M-AANBI.

3.6. Case presentation

Herein, we highlight 2 cases of gastric neoplasm. The first case involved an 80-year-old woman with gastric adenoma. Her tumor was located within the greater curvature of the gastric antrum (diameter: 5 mm); it was of an elevated macroscopic type with a whitish color (Fig. 5A). M-NBI exhibited irregular microvascular and microsurface patterns with a visible demarcation line, suggestive of carcinoma (Fig. 5B). In comparison, M-AANBI demonstrated a slit microsurface pattern with a visible demarcation line, suggestive of an adenoma (Fig. 5C). Histopathologically, the tumor was diagnosed as an adenoma after ESD (Fig. 5D).

The second case involved a 75-year-old man with gastric carcinoma. Initially diagnosed as an adenoma by biopsy, his tumor was located within the lesser curvature of the gastric angle (diameter: 18 mm); it was of an elevated macroscopic type with a reddish color (Fig. 5E). M-NBI exhibited irregular microvascular and regular microsurface patterns with a visible demarcation line, suggestive of an adenoma (Fig. 5F). In comparison, M-AANBI demonstrated an irregular microsurface pattern with a visible demarcation line, suggestive of carcinoma (Fig. 5G). Histopathologically, the tumor was diagnosed as a well-differentiated adenocarcinoma after ESD (Fig. 5H).

These 2 gastric lesions had different predictions based on M-NBI and M-AANBI. In the second case, the lesion was <20 mm and had regular M-NBI findings; thus, carcinoma mimicked adenoma. Notably, M-AANBI was crucial to obtaining an accurate preoperative diagnosis in this case.

4. Discussion

We performed a retrospective analysis of gastric carcinoma prevalence and compared the diagnostic performances of M-NBI and M-AANBI in terms of distinguishing carcinomas from adenomas in lesions diagnosed by M-AANBI using endoscopic forceps biopsy. The prevalence of gastric carcinoma was 40.8%, and 3 lesions were diagnosed as submucosal invasive carcinomas. Subsequently, M-AANBI displayed a significantly higher diagnostic accuracy than M-NBI for distinguishing carcinomas from adenomas.

The outcome of ESD for early gastric carcinomas (T1a) is reportedly equivalent to that of surgical resection.[18] ESD is a feasible therapeutic method for treating early gastric carcinomas. Endoscopic forceps biopsy is an important method for differentiating between gastric adenomas and carcinomas. Nonetheless, we frequently experienced inconsistencies between the histopathological findings from biopsy and resected specimens. Biopsy specimens are relatively small and can lead to underdiagnosis because they often do not contain the malignant components of the lesion; moreover, this lack of representation has been reported in existing literature.[4,5] Thus, an endoscopic repeat examination and resection should be considered for gastric adenomas diagnosed by biopsy.

M-NBI is an effective diagnostic method for predicting the histological characteristics of gastric neoplasms by providing a distinct visualization of microvascular and microsurface patterns.[2,9,10,15,19] M-NBI often displays both mucosal microvascular and microsurface patterns simultaneously, thereby making it occasionally difficult to distinguish carcinomas from adenomas. Shibagaki et al reported that M-NBI did not display an advantage over WLE in terms of overall diagnostic accuracy.[14]

Initially, M-AA was designed to improve the diagnosis of Barrett esophagus[20] because it is difficult to recognize an intestinalized epithelium in a columnar-lined esophagus using WLE. Barrett mucosa was classified into 3 types according to M-AA.[21] Previously, we established a classification system for gastric mucosa using M-AA.[12,13] Adenomas were principally characterized by the following 2 recognizable patterns of the surface structure: slit and gyrus/villous. Conversely, carcinomas were principally characterized by irregular and destructive patterns. Differentiated adenocarcinomas exhibited an irregular microsurface pattern, whereas signet-ring cell carcinomas and poorly differentiated adenocarcinomas primarily exhibited a destructive pattern.

M-AANBI masks the microvascular pattern of gastric lesions because of the aceto-whitening reaction. However, it enables clear visualization of microsurface patterns and simplifies its findings, unlike WLE and M-NBI. Therefore, M-AANBI improves the diagnostic accuracy[14] and demarcation recognition[22] of gastric neoplasms, compared with WLE and M-NBI. Similarly, M-AANBI displayed significantly higher diagnostic accuracy than M-NBI and substantial inter-observer agreement between both experts and non-experts in this study. According to the results of M-AANBI diagnosis, endoscopists are required to use M-AANBI for an accurate diagnosis of gastric adenomatous lesions initially diagnosed by biopsy.
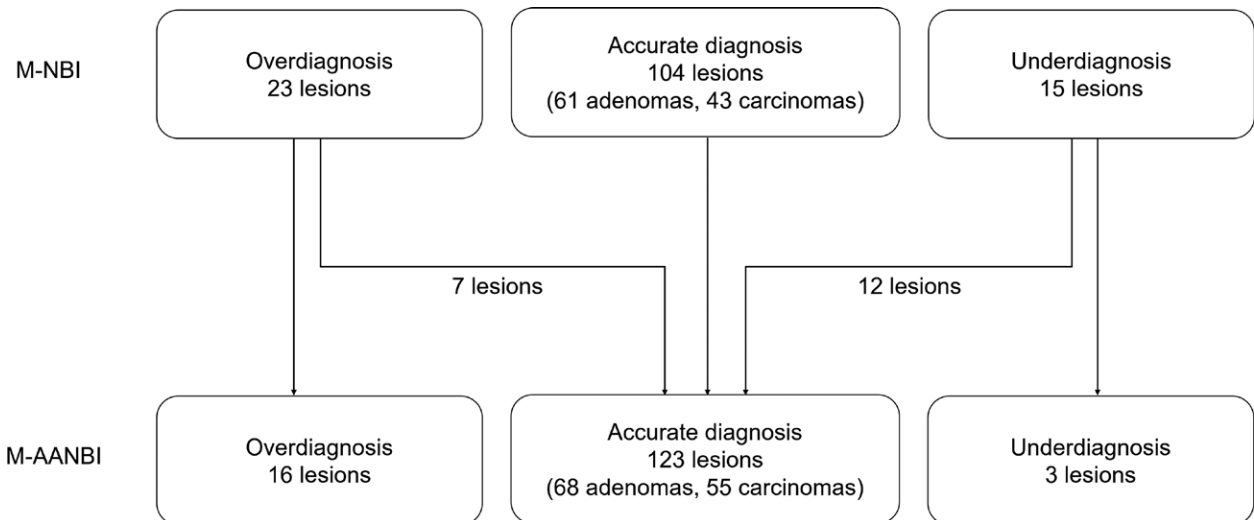
Figure 4. The number of misdiagnoses by M-NBI and M-AANBI. The lesions diagnosed accurately by M-NBI were not misdiagnosed by M-AANBI. Overdiagnosis refers to the endoscopic misdiagnosis of a pathologic adenoma as a carcinoma; underdiagnosis refers to the endoscopic misdiagnosis of a pathologic carcinoma as an adenoma. M-AANBI = magnifying endoscopy with acetic acid and narrow-band imaging, M-NBI = magnifying endoscopy with narrow-band imaging.
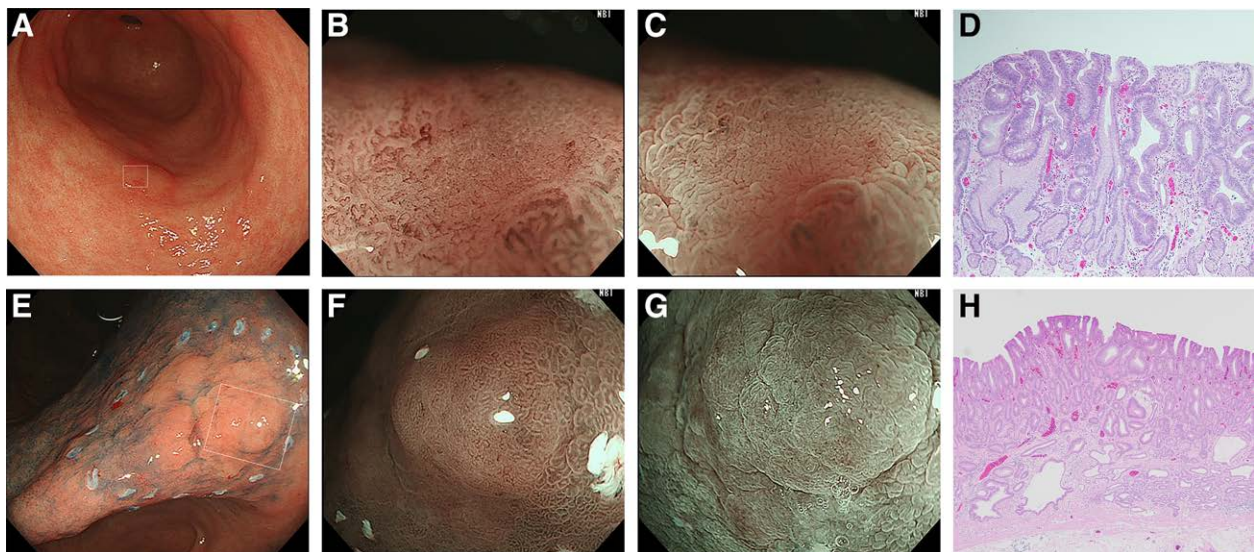

Figure 5. Endoscopic images of 2 cases of gastric neoplasms. (A) Case 1: WLE displaying a normochromic lesion on the greater curvature of the antrum. (B) Case 1: M-NBI displaying irregular microvascular with obscure microsurface patterns and a demarcation line suggestive of carcinoma. (C) Case 1: M-AANBI showing a slit pattern with a demarcation line, suggestive of an adenoma. (D) Case 1: A pathological diagnosis of adenoma. (E) Case 2: WLE displaying a normochromic lesion on the lesser curvature of the gastric angle after a circumferential marking during endoscopic submucosal dissection. (F) Case 2: M-NBI displaying regular microvascular and microsurface patterns with a demarcation line, suggestive of an adenoma. (G) Case 2: M-AANBI displaying an irregular pattern with a demarcation line, suggestive of a carcinoma. (H) Case 2: A pathological diagnosis of adenocarcinoma. M-AANBI = magnifying endoscopy with acetic acid and narrow-band imaging, M-NBI = magnifying endoscopy with narrow-band imaging, WLE = white-light endoscopy.

Regarding the long-term follow-up, 97% of adenoma lesions displayed no histological change at a median follow-up of 4.7 years.[1] In addition, gastric ESD has several challenges as a treatment strategy for adenomas, including the need for a high technical skill level, risks of long-term sedation, long procedure time, and a high incidence of adverse events. Therefore, an observation strategy without resection for definite gastric adenomas may be considered a management option, particularly for older adults. An accurate diagnosis by M-AANBI may be essential for selecting gastric adenoma management strategies for older adults, that is, ESD or observation.

This study has some limitations. First, this retrospective study used selective endoscopic images. Further, a selection bias toward high-quality images was present. However, considering that

endoscopists can observe all lesions in real-time clinical practice, the use of high-quality images should be acceptable. Further experience with more cases is required to improve the diagnostic performances of such endoscopic procedures. However, a further prospective validation study that examines the effect of M-AANBI combined with M-NBI on the identification of carcinoma from gastric adenomas initially diagnosed by endoscopic biopsy is required to establish our results. For gastric lesions, M-NBI will be followed by M-AANBI. Diagnoses using these 2 methods should be recorded in real-time. Eventually, comparisons between the endoscopic and pathological findings are necessitated. Second, an image selection bias could exist in the agreement study. We minimized the bias to the maximum possible extent by selecting appropriate images for all 142 lesions. Third,

a demarcation line was essential for diagnosing adenomas; however, no previous studies have used a demarcation line in M-NBI for adenoma diagnosis, thus necessitating a prospective study. However, an adenoma is an epithelial neoplastic lesion similar to gastric carcinoma; therefore, it may display a demarcation line, despite being relatively indistinct compared to definite carcinoma.

In conclusion, carcinoma was prevalent in 40.8% of gastric lesions initially diagnosed as adenomas by forceps biopsy. M-AANBI may be better than M-NBI in distinguishing carcinomas from adenomas. Endoscopists are required to consider endoscopic resection for gastric adenomas diagnosed by biopsy upon observing an irregular microsurface pattern by M-AANBI. Future prospective studies are required to validate the diagnostic accuracy of M-AANBI.

Acknowledgments

Author contributions

Conceptualization: Yuhei Umeda, Kyosuke Tanaka.
Data curation: Yuhei Umeda, Yohei Ikenoyama, Toru Ogura.
Formal analysis: Toru Ogura, Satoshi Tamaru.
Investigation: Yuhei Umeda, Yohei Ikenoyama.
Methodology: Yuhei Umeda.
Supervision: Kyosuke Tanaka, Hayato Nakagawa, Isao Tawara.
Validation: Yohei Ikenoyama, Masaki Katsurahara, Hayato Nakagawa, Isao Tawara.
Visualization: Kyosuke Tanaka.
Writing – original draft: Yuhei Umeda.
Writing – review & editing: Kyosuke Tanaka, Yohei Ikenoyama, Yasuhiko Hamada, Hiroki Yukimoto, Reiko Yamada, Junya Tsuboi, Misaki Nakamura, Masaki Katsurahara, Noriyuki Horiki, Toru Ogura, Satoshi Tamaru, Hayato Nakagawa, Isao Tawara.

References

[1] Yamada H, Ikegami M, Shimoda T, et al. Long-term follow-up study of gastric adenoma/dysplasia. Endoscopy. 2004;36:390–6.
[2] Nonaka K, Arai S, Ban S, et al. Prospective study of the evaluation of the usefulness of tumor typing by narrow band imaging for the differential diagnosis of gastric adenoma and well-differentiated adenocarcinoma. Dig Endosc. 2011;23:146–52.
[3] Muehldorfer SM, Stolte M, Martus P, et al. Diagnostic accuracy of forceps biopsy versus polypectomy for gastric polyps: a prospective multicentre study. Gut. 2002;50:465–70.
[4] Kim MK, Jang JY, Kim JW, et al. Is lesion size an independent indication for endoscopic resection of biopsy-proven low-grade gastric dysplasia? Dig Dis Sci. 2014;59:428–35.
[5] Kim YJ, Park JC, Kim JH, et al. Histologic diagnosis based on forceps biopsy is not adequate for determining endoscopic treatment of gastric adenomatous lesions. Endoscopy. 2010;42:620–6.
[6] Noh CK, Jung MW, Shin SJ, et al. Analysis of endoscopic features for histologic discrepancies between biopsy and endoscopic submucosal dissection in gastric neoplasms: 10-year results. Dig Liver Dis. 2019;51:79–85.
[7] Jung MK, Jeon SW, Park SY, et al. Endoscopic characteristics of gastric adenomas suggesting carcinomatous transformation. Surg Endosc. 2008;22:2705–11.
[8] Kono Y, Takenaka R, Kawahara Y, et al. Chromoendoscopy of gastric adenoma using an acetic acid indigocarmine mixture. World J Gastroenterol. 2014;20:5092–7.
[9] Ezoe Y, Muto M, Uedo N, et al. Magnifying narrowband imaging is more accurate than conventional white-light imaging in diagnosis of gastric mucosal cancer. Gastroenterology. 2011;141:2017–2025.e3.
[10] Nonaka T, Inamori M, Honda Y, et al. Can magnifying endoscopy with narrow-band imaging discriminate between carcinomas and low grade adenomas in gastric superficial elevated lesions? Endosc Int Open. 2016;4:E1203–10.
[11] Tamura N, Sakaguchi Y, Furutani W, et al. Magnifying endoscopy with narrow-band imaging is useful in differentiating gastric cancer from matched adenoma in white light imaging. Sci Rep. 2022;12:8349.
[12] Tanaka K, Toyoda H, Kadowaki S, et al. Features of early gastric cancer and gastric adenoma by enhanced-magnification endoscopy. J Gastroenterol. 2006;41:332–8.
[13] Tanaka K, Toyoda H, Kadowaki S, et al. Surface pattern classification by enhanced-magnification endoscopy for identifying early gastric cancers. Gastrointest Endosc. 2008;67:430–7.
[14] Shibagaki K, Amano Y, Ishimura N, et al. Diagnostic accuracy of magnification endoscopy with acetic acid enhancement and narrow-band imaging in gastric mucosal neoplasms. Endoscopy. 2016;48:16–25.
[15] Muto M, Yao K, Kaise M, et al. Magnifying endoscopy simple diagnostic algorithm for early gastric cancer (MESDA-G). Dig Endosc. 2016;28:379–93.
[16] Japanese Gastric Cancer Association. Japanese classification of gastric carcinoma: 3rd English edition. Gastric Cancer. 2011;14:101–12.
[17] Kanada Y. Investigation of the freely available easy-to-use software "EZR" for medical statistics. Bone Marrow Transpl. 2013;48:452–8.
[18] Hasuike N, Ono H, Boku N, et al. A non-randomized confirmatory trial of an expanded indication for endoscopic submucosal dissection for intestinal-type gastric cancer (cT1a): the Japan Clinical Oncology Group study (JCOG0607). Gastric Cancer. 2018;21:114–23.
[19] Yamada S, Doyama H, Yao K, et al. An efficient diagnostic strategy for small, depressed early gastric cancer with magnifying narrow-band imaging: a post-hoc analysis of a prospective randomized controlled trial. Gastrointest Endosc. 2014;79:55–63.
[20] Guelrud M, Herrera I, Essenfeld H, et al. Enhanced magnification endoscopy: a new technique to identify specialized intestinal metaplasia in Barrett's esophagus. Gastrointest Endosc. 2001;53:559–65.
[21] Toyoda H, Rubio C, Befrits R, et al. Detection of intestinal metaplasia in distal esophagus and esophagogastric junction by enhanced-magnification endoscopy. Gastrointest Endosc. 2004;59:15–21.
[22] Kadowaki S, Tanaka K, Toyoda H, et al. Ease of early gastric cancer demarcation recognition: a comparison of four magnifying endoscopy methods. J Gastroenterol Hepatol. 2009;24:1625–30.